AIP Journal of Applied Physics

A semi-empirical equation for the response time of in-plane switching liquid crystal display and measurement of twist elastic constant

Daming Xu, Fenglin Peng, Guanjun Tan, Juan He, and Shin-Tson Wu

Citation: Journal of Applied Physics **117**, 203103 (2015); doi: 10.1063/1.4921872
View online: http://dx.doi.org/10.1063/1.4921872
View Table of Contents: http://scitation.aip.org/content/aip/journal/jap/117/20?ver=pdfcov
Published by the AIP Publishing

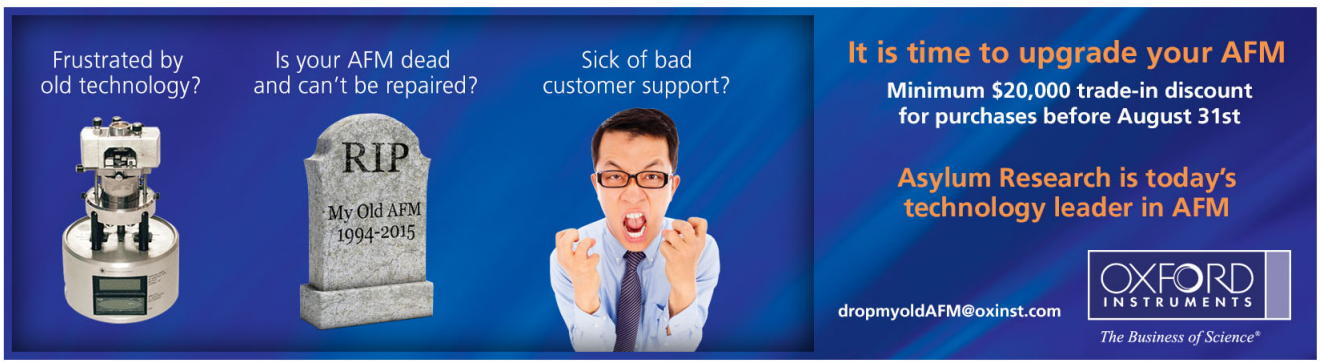

A semi-empirical equation for the response time of in-plane switching liquid crystal display and measurement of twist elastic constant

Daming Xu, Fenglin Peng, Guanjun Tan, Juan He, and Shin-Tson Wu[a)]
College of Optics and Photonics, University of Central Florida, Orlando, Florida 32816, USA

(Received 27 March 2015; accepted 19 May 2015; published online 29 May 2015)

A semi-empirical equation is developed to characterize the optical decay time of in-plane switching (IPS) and fringe field switching (FFS) liquid crystal displays. This equation takes the effects of elastic constants, cell gap, liquid crystal material, rubbing angle, and anchoring strength into account simultaneously. Good agreement between simulation and experiment is obtained. Moreover, this equation can be used to measure the twist elastic constant K_{22} of liquid crystals. The measured temperature-dependent K_{22} values of 5CB agree well with previously published results. Hence, our equation not only describes the response time of IPS and FFS cells but also provides a simple yet accurate method to determine the twist elastic constant of liquid crystal materials. © *2015 AIP Publishing LLC*. [http://dx.doi.org/10.1063/1.4921872]

I. INTRODUCTION

Liquid crystal displays (LCDs), such as smartphones, tablets, and large-size TVs, have become indispensable in our daily lives.[1–3] Three commonly used LC modes are twisted nematic (TN),[4,5] vertical alignment (VA),[6,7] and in-plane switching (IPS)[8–11] including fringe field switching (FFS).[12–14] In TN, VA, and homogeneous cells, the longitudinal electric field is uniform so that their dynamic response can be solved analytically under small angle and single elastic constant approximations.[15,16] However, in IPS and FFS modes, the fringe field is not uniform in neither lateral nor longitudinal direction.[17] As a result, it is quite difficult to derive an analytical solution to describe the dynamic behavior of LC directors. A common approach to obtain the optical response time (mainly decay time τ_d, since rise time is more complicated as it also depends on the applied voltage) is either through numerical solution or using following approximated equation:

$$\tau_d \sim \tau_0 = \frac{\gamma_1 d^2}{K_{22}\pi^2}, \tag{1}$$

where γ_1 is the rotational viscosity, d is the cell gap, and K_{22} is the twist elastic constant. Eq. (1) is assumed to be analogous to the analytical solution of homogeneous cell (with splay elastic constant K_{11}) and VA (with bend elastic constant K_{33}) cell,[18] but without rigorous proof. Qualitatively, the decay time is indeed proportional to the visco-elastic coefficient (γ_1/K_{22}) and d^2, but quantitatively the error is about 25%–30%, as will be shown later.

Another challenge as shown in Eq. (1) involves the accurate measurement of K_{22}. For splay elastic constant K_{11} and bend elastic constant K_{33}, there are sufficiently accurate and simple measurement methods based on the work of Gruler.[19] However, the methods for determining twist constant K_{22} are less straightforward and require much more complicated experimental setups such as magnetic fields,[20] a torsion pendulum,[21] optical light scattering,[22] the guided mode techniques,[23] the wedge cell or pi-cell,[24,25] etc., among which the magnetic field method has the highest accuracy. These methods require either complex measurement equipment or elaborate fitting routine, thus rendering the measurement of K_{22} less routinely. Hence, there is an urgent need to develop a simple yet accurate method to measure K_{22}.

In this article, we investigate the optical decay time of IPS cells by both simulation and experiment, from which we develop a semi-empirical equation to calculate the decay time accurately. The dependence of optical decay time on the elastic constant, cell gap, LC material properties, rubbing, and anchoring conditions are investigated. Based on the obtained equation, the K_{22} value can be measured in a simple way. We measure the K_{22} values of 5CB at different temperatures and obtain good agreement with literature results. Thus, our semi-empirical equation serves two important objectives: (1) it reliably describes the optical response time of IPS and FFS cells, and (2) it provides a simple method to measure the twist elastic constant accurately. Based on this method, we study the visco-elastic coefficient for various materials and establish guidelines for future material optimization.

II. SIMULATION RESULTS

The dynamic decay processes of both IPS and FFS modes are computed by using commercial simulator TechWiz LCD (Sanayi, Korea). The computations can be divided into two steps: (1) find the LC director distribution; and (2) simulate electro-optic performance. Three-dimensional (3D) finite element method[26,27] is used to numerically analyze the full-space distribution of LC directors. Then, the electro-optic performance are calculated by the extended 2×2 Jones matrix method. In general, this 3D simulator is very accurate and reliable compared to experimental results.

In our simulations, IPS and FFS cells with various electrode width (W) and gap (G) are investigated, such as IPS-5/5 ($W = G = 5$ μm), FFS-2/3 ($W = 2$ μm, $G = 3$ μm),

[a)]Electronic mail: swu@ucf.edu

etc. The alignment layer is 80-nm thick polyimide (PI) with a dielectric constant of 3.8 for all simulated cells. In the FFS cells, the passivation layer between the pixel and common electrodes is Si_3N_4 ($\varepsilon = 7.5$) whose thickness is 150 nm. Several LC materials are studied and their physical properties listed in Table I. Here, HAI (HAI-653265, HCCH, China), DIC-LC2 (DIC, Japan), and ZLI-1132 (Merck, Germany) are LCs with positive dielectric anisotropy ($+\Delta\varepsilon$); while HAV (HAV-634117, HCCH, China), MX-40593 (LC Vision, USA), and MLC-6882 (Merck, Germany) are negative ($-\Delta\varepsilon$) LCs. The K_{22} values of three positive LCs are provided by the vendors, whereas those of the three negative LCs are unknown and need to be measured.

A. Elastic constant effect

As shown in Eq. (1), τ_d is proportional to the reciprocal of K_{22}. Here, we revisit the elastic constant effect by varying each elastic constant within a reasonable range (K_{11} and K_{33}: 5–17 pN, K_{22}: 3–12 pN) while keeping all other material parameters unchanged based on two base materials HAI ($+\Delta\varepsilon$) and MLC-6882 ($-\Delta\varepsilon$). On the device side, for the purpose of achieving low driving voltage, the homogeneous rubbing angle is set at 80° and 10° *w.r.t.* the stripe electrodes axis for IPS and FFS cells using a negative (namely, n-IPS or n-FFS) and positive (namely, p-IPS or p-FFS) LC, respectively. The cell gap is optimized at $\lambda = 550$ nm with $d{\cdot}\Delta n = 360$ nm for negative cells and 380 nm for positive cells to obtain high transmittance.[28] Strong anchoring energy ($W = 10^{-3}$ J/m^2) applies to all the LC cells. The LC cell is further interposed between two crossed linear polarizers with bottom polarizer's transmission axis parallel to the LC rubbing direction. To simulate the dynamic relaxation process, each cell is first biased at its corresponding on-state voltage, then the voltage is removed and the decay time τ_d for 90%–10% transmittance change is calculated from the transient transmittance decay curve.

Figure 1 depicts the dependence of τ_d on each elastic constant for the IPS-5/5 cell. Due to the limitation of space, here, we only show the simulation results of p-IPS cell, but the n-IPS and FFS cells exhibit the same trend. It clearly shows that τ_d remains unchanged as K_{11} and K_{33} vary, indicating that τ_d is independent of K_{11} and K_{33} although the tilt angles are fairly large in p-IPS and p-FFS cells.[13] This is because the tilt angles do not contribute to the transmittance; thus, the relaxation of tilted LC directors is not explicitly manifested by the transmittance change during the decay process. In contrast, a different trend is exhibited for the twist elastic constant: τ_d decreases dramatically as K_{22} increases. Here, we use the reciprocal function to fit the simulation results and the fitted curve is shown as the magenta solid line in Fig. 1. Good agreement between fitting curve and discrete circles indicates the dependence of τ_d on the elastic constant follows:

$$\tau_d \sim \frac{1}{K_{22}}, \tag{2}$$

even though the electric fields and LC directors distribution in the IPS and FFS cells are quite non-uniform.[12,13,17]

TABLE I. Physical properties of the six LC mixtures studied (T = 23 °C, $\lambda = 633$ nm, and f = 1 kHz).

LC	T_C (°C)	$\Delta\varepsilon$	Δn	γ_1 (mPa s)	K_{22} (pN)
HAI	80.0	2.4	0.096	42.8	7.8
DIC-LC2	75.5	1.7	0.117	32.0	6.5
ZLI-1132	71.0	12.0	0.137	159.8	6.3[25]
HAV	89.5	−3.79	0.108	98.5	…
MX-40593	79.3	−2.47	0.101	64.4	…
MLC-6882	69.0	−3.1	0.097	108.0	…

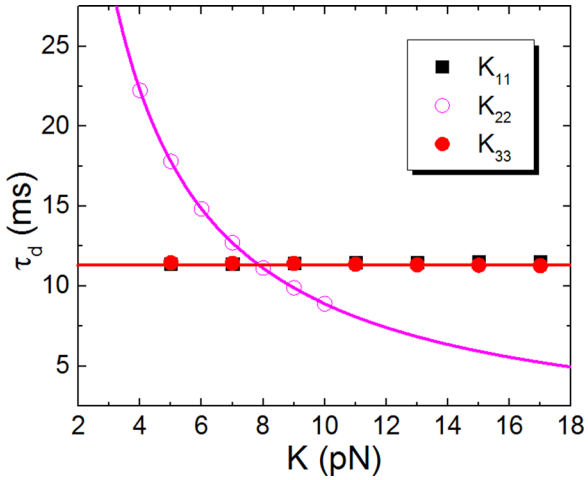

FIG. 1. Dependence of decay time on three elastic constants for the IPS-5/5 cell (LC mixture: HAI).

B. Cell gap effect

From previous studies,[29] the decay time of a LC device τ_d is proportional to d^x, where d is the cell gap and x is an exponent determined by the anchoring energy and cell gap. Under strong anchoring condition, the exponent x approaches 2. Here, we simulate the decay time τ_d of IPS and FFS cells with cell gaps varying in a reasonable range for display applications (2.5–4 μm), and the simulation results are plotted in Fig. 2. As we can see, τ_d increases as d^2 increases. To describe this trend, we use a linear function to

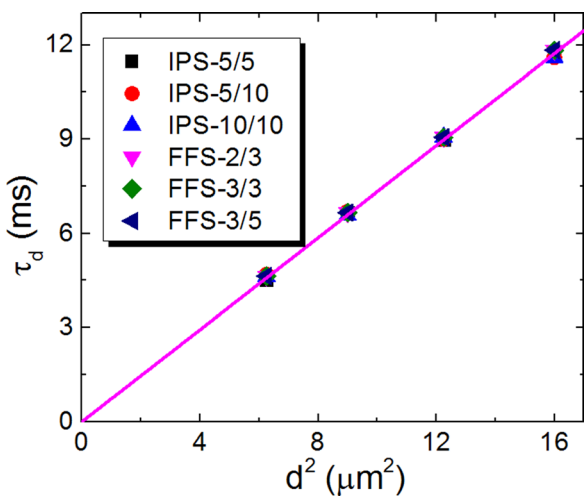

FIG. 2. Dependence of decay time on the cell gap for various p-IPS and p-FFS cells (LC: HAI).

fit the simulated results, as plotted by the magenta line. A good agreement is obtained between the fitting curve and simulated data, indicating that dependence of τ_d on the cell gap can be written as

$$\tau_d \sim d^2. \tag{3}$$

Hence, together with the discussions above, we can write the decay time as a function of cell gap, rotational viscosity, and twist elastic constant

$$\tau_d = A \cdot \frac{\gamma_1 d^2}{K_{22}\pi^2}. \tag{4}$$

Here, A is a proportional constant, as represented by the slope of the fitting curve in Fig. 2. Also shown in Fig. 2 is that A is independent of electrode dimension, showing that A may only depend on other cell properties (e.g., rubbing, anchoring, etc.) or LC material properties, as will be discussed later.

C. LC material dependence

The LC material dependence of A is investigated by simulating the optical decay time of IPS and FFS cells employing different materials from Table I. For each LC, K_{22} is varied within a reasonable range (4–8 pN). Table II compares the simulated A values of the p-IPS cells using three positive LCs. As we can see, for all three LC materials, the proportionality constant A is independent of K_{22} and their A values are all in the range of 1.287 ± 0.007 (error: $\pm 0.54\%$). Hence, A is independent of LC material properties. This is an attractive feature, as it means that Eq. (4) is universally applicable to all IPS and FFS cells no matter what LC material is employed.

D. Rubbing angle effect

In addition to the effects of material properties discussed above, the dependence of A on the device parameters such as rubbing conditions are also investigated. The typical rubbing angle φ_0 is 80° and 10° *w.r.t.* the grid electrodes for LC cells employing negative and positive $\Delta\varepsilon$ LC, respectively.[13] For different fabrication techniques, the rubbing angle may vary in the range of $\varphi_0 \pm 4°$.[30,31] Rubbing angles not being set in this range would incur either increased on-state voltage or slower rise time, both of which are undesirable. In our studies, we simulate the A values for p-IPS and n-IPS cells with rubbing angle φ varying in an even wider range ($\varphi_0 \pm 8°$), as listed in Table III. As we can see, as rubbing angle φ varies, the decay time constant A remains almost unchanged for both p-IPS and n-IPS cells, which is different from rise time. Taking p-IPS cell as an example, as φ decreases, the rise time becomes slower due to the reduced torque on LC directors exerted by the electric field. At the full-bright state, the twist angle should occur at $\sim\varphi + 45°$ in order to obtain maximum phase retardation.[12,13] Hence, the deviation of LC directors from the rubbing angle is same for LC cells with different rubbing angles. Upon the removal of the on-state voltage, the relaxation torque exerted by the surface anchoring is almost the same. As a result, the decay time is nearly the same for all these cells and A is not affected by the rubbing angles.

E. Anchoring energy effect

The anchoring energy (W) in an LC device has profound impact on the electro-optical properties of the device. In practical applications, different anchoring conditions can be used depending on the objectives: strong anchoring is usually defined as $W \geq 10^{-3}$ J/m^2, weak anchoring is typically in the range of $W \leq 10^{-5}$ J/m^2, and medium anchoring is in between.[32] The anchoring energy tend to anchor the LC directors near the substrates on their easy axis and the impact of the anchoring decreases as it goes deeper into the LC bulk. When the applied voltage exceeds the Freederisckz transition threshold, the LC directors are reoriented by the electric field. An important parameter characterizing the surface anchoring strength is the extrapolation length given by $L \sim K/W$.[29,32,33] The extrapolation length parameterizes the distance from the real surface where the director would coincide with the original "easy axis" orientation and can be interpreted as the extension of the LC cell gap.[34] For example, an infinity anchoring ($W \rightarrow \infty$) means no extension since $L = 0$; as a result, the directors coincide with easy axis orientation near the surface. On the other hand, weak anchoring leads to a large L, thus resulting in a large extension of the LC cell gap.

When the extrapolation length is taken into account, the effective cell gap becomes

$$d' = d + 2L. \tag{5}$$

Then, Eq. (4) can be further modified to describe the LC decay time when W is finite by replacing the physical cell gap d with the effective cell gap d', as shown below

TABLE II. Simulated A values for p-IPS cells employing different LC mixtures.

K_{22} (pN)	HAI	DIC-LC2	ZLI-1132
4	1.289	1.288	1.286
5	1.288	1.280	1.287
6	1.288	1.284	1.285
7	1.291	1.286	1.290
8	1.292	1.284	1.294

TABLE III. Simulated A values for p- and n-IPS -5/5 cells employing HAI and MLC-6882, respectively.

$\varphi - \varphi_0$	p-IPS	n-IPS
−8°	1.284	1.281
−4°	1.286	1.286
0°	1.288	1.287
4°	1.289	1.292
8°	1.291	1.289

$$\tau_d = A_0 \cdot \frac{\gamma_1}{K_{22}\pi^2} \cdot (d+2L)^2 = A_0 \cdot \frac{\gamma_1}{K_{22}\pi^2} \cdot \left(d^2 + \frac{4dK_{22}}{W} + \frac{4K_{22}^2}{W^2}\right), \quad (6)$$

where A_0 is proportionality constant under the infinity anchoring condition ($W \rightarrow \infty$). From Eq. (6), $\tau_d \sim d^2$ if $2L \ll d$, i.e., strong anchoring energy (as shown in Sec. II B), then the anchoring energy is negligible and Eq. (5) can be simplified to Eq. (4). For a medium anchoring energy, $2K_{22}/W$ is not negligible and we have to consider the anchoring energy term in the right hand of Eq. (6). Higher anchoring energy would exert a stronger torque on the LC directors during the relaxation process and lead to a faster decay time.

To validate the derivations above, we simulate the decay time of p-IPS-5/5 cell employing HAI under different anchoring conditions and the calculated A values are plotted as magenta dots in Fig. 3. It clearly shows that A decreases dramatically as the anchoring energy increases and finally saturates in the strong anchoring region. Here, we fit the discrete dots in Fig. 3 with following equation:

$$A = A_0 \cdot \left(d^2 + \frac{4dK_{22}}{W} + \frac{4K_{22}^2}{W^2}\right), \quad (7)$$

and the fitting results are plotted as the blue solid line. Good agreement is obtained between the discrete dots and fitting curve, indicating that Eqs. (6) and (7) well describe the anchoring energy effects in IPS and FFS cells. The proportionality constant under infinity anchoring condition ($W \rightarrow \infty$) is $A_0 = 1.277$.

In brief, the proportionality constant A is independent of rubbing angle, LC material, cell gap, etc. It is only determined by the anchoring energy and Eq. (6) is universally applicable to describe the decay time of IPS and FFS cells under different anchoring conditions. Next, we will validate this proportionality constant A by experiment.

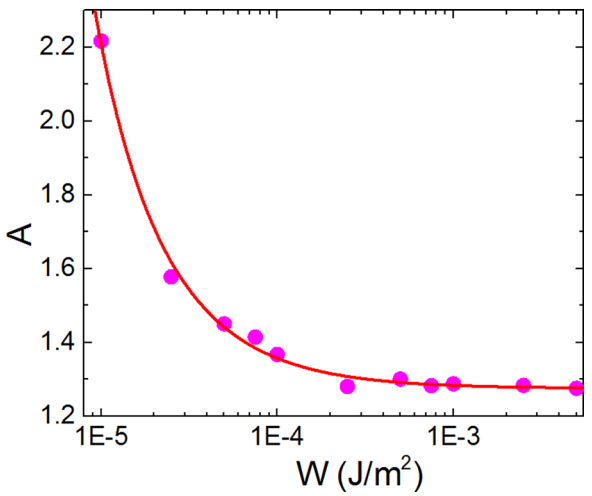

FIG. 3. Dependence of A on the anchoring energy for p-IPS-5/5 cell (Rubbing angle $\varphi = 80°$, LC: HAI).

III. EXPERIMENTAL RESULTS

A. Experiment vs. simulation

In experiment, we prepare three IPS-10/10 cells (from Instec, USA) using the positive LCs listed in Table I. In these cells, both top and bottom substrates are coated with a thin PI layer. The PI layer is mechanically rubbed to provide strong anchoring. The cell gap is measured by counting the Fabry-Perot interference fringes from a spectrometer, as listed in Table IV. The cell is then sandwiched between two crossed linear polarizers with the bottom polarizer's transmission axis parallel to the LC rubbing direction. A He-Ne laser ($\lambda = 632.8$ nm) is used as the probing beam. We first measure the voltage-dependent transmittance curve and then record the transient transmittance decay process from the full-bright to dark state with a digital oscilloscope. The measured optical decay times are also included in Table IV. From the material parameters listed in Table I, we also calculated the theoretical τ_0. Then, the proportionality constant A is calculated for all three materials, as shown in the last column of Table IV. We find that A is in the range of 1.238 ± 0.016 (error: $\pm 1.29\%$) from experiments. Compared to the simulated value ($A = 1.287$), the experimental value is 3.41% smaller, which is acceptable considering the discrepancy between simulation and experiment. Therefore, our experiment validates that there is indeed a non-unity proportionality constant A that is universally applicable to different LC materials. More importantly, a semi-empirical equation is obtained to describe the optical decay time of IPS cells

$$\tau_d = 1.238 \cdot \frac{\gamma d^2}{K_{22}\pi^2}. \quad (8)$$

B. Measurement of 5CB

To further verify the applicability of our semi-empirical equation, we measure the K_{22} values of the well-studied 5CB under different temperatures and then compared our data with published results. We inject 5CB into an IPS-10/10 cell with same conditions as described above. The response time of the IPS cell is then measured at different temperatures and the temperature-dependent K_{22} values were calculated using Eq. (8).

The measured temperature-dependent K_{22} values of 5CB are depicted as the blue diamonds in Fig. 4. For comparison purpose, we also include the measured data by Breddels and Mulkens[35] (red dots) using the magnetic field measurement method. Meanwhile, we also calculate the K_{22} values from the K_{11}/K_{22} and K_{33}/K_{22} data by Hara *et al.*[36] along with the values of K_{11} and K_{33} measured by Bradshaw

TABLE IV. Measured cell gap, optical decay time, and A values for three IPS-10/10 cells. (T = 23 °C, $\lambda = 633$ nm, and f = 1 kHz).

LC	d (μm)	τ_0 (ms)	τ_d (ms)	A
HAI	3.71	7.65	9.35	1.222
DIC-LC2	3.23	5.20	6.47	1.244
ZLI-1132	3.69	34.99	43.88	1.254

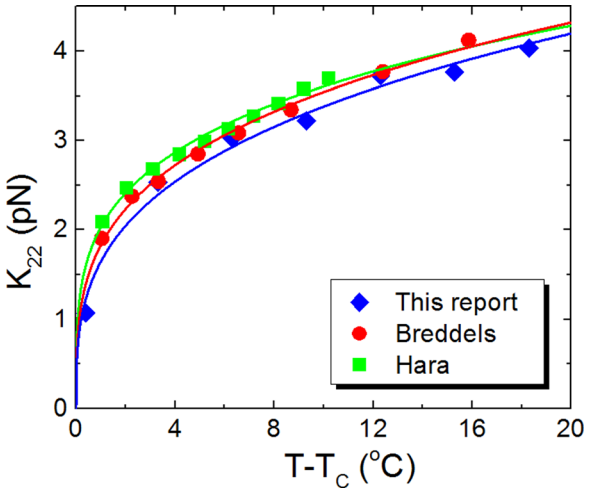

FIG. 4. Temperature-dependent K_{22} values of 5CB.

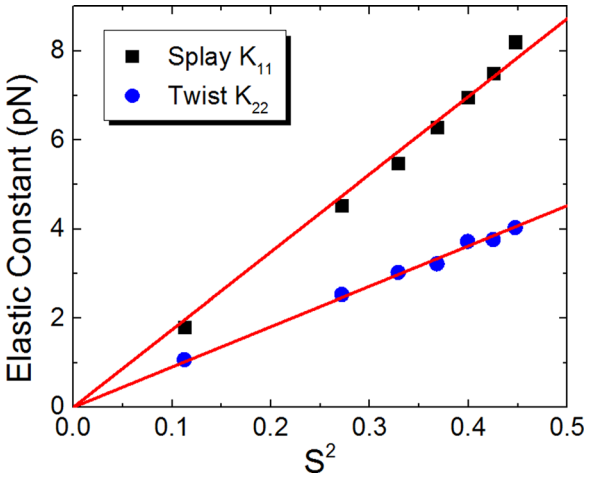

FIG. 5. K_{11} and K_{22} as a function of order parameter for 5CB.

and Raynes.[37] These values are plotted as the green squares in Fig. 4. As we can see, our measured data agree well with literature results, thus proving again that Eq. (8) is accurate for determining K_{22}.

The temperature-dependent K_{22} values measured by our method are further verified by the order parameter S, which parameterizes the average directions of the long axes for the rod-like molecules and can be described by Haller's semi-empirical equation[38,39]

$$S = (1 - T/T_C)^{\beta}. \tag{9}$$

Here, T_C is the clearing point of the LC material and β is a material constant. The order parameter affects the physical properties of LC material, e.g., birefringence Δn and elastic constant K_{ii} are related to order parameter by[16,32]

$$\Delta n = \Delta n_0 \cdot S, \tag{10}$$

$$K_{ii} = c_i \cdot S^2, \tag{11}$$

where Δn_0 and c_i are the extrapolated birefringence and elastic constant at $T = 0\,\mathrm{K}$.

In experiments, we also measure the birefringence of 5CB at different temperatures. The temperature-dependent birefringence is then fitted with Eqs. (9) and (10). The T_C of 5CB is 308.3 K, and we obtain $\beta = 0.142$, which is consistent with previous results.[40] Then, we plot the measured K_{11} and K_{22} as functions of S^2, as shown in Fig. 5. The measured data increase linearly with S^2, and this trend is fitted with Eq. (11). The fitting parameters are as follows: $c_1 = 17.45\,\mathrm{pN}$ and $c_1 = 9.10\,\mathrm{pN}$. Good agreement is obtained between the linear fitting curve and measured data, indicating that our measurement method is reliable.

C. Material development

Recently, extensive efforts have been devoted to achieve faster response time for IPS and FFS LCDs,[41–45] among which lowering the visco-elastic coefficient γ_1/K_{22} of LC is a very effective method from the material side. Since γ_1 can be measured very easily, low-viscosity materials are well studied in material designs.[45] In contrast, due to the difficulties in K_{22} measurement, the impact of K_{22} is sometimes overlooked. Now, with the verified semi-empirical equation presented above, we are able to accurately evaluate the visco-elastic coefficient for IPS and FFS LC materials.

We first measure the K_{22} values of the negative materials listed in Table I. Their K_{22} values are found to be 6.4 pN (HAV), 5.4 pN (MX-40593), and 7.9 pN (MLC-6882), respectively. To compare their performance, we plot their visco-elastic coefficient γ_1/K_{22} in Fig. 6, as shown by the magenta squares. Here, two other negative LC materials with higher dielectric anisotropy from Merck, namely, MLC-6608 ($\Delta\varepsilon = -4.2$) and MLC-6609 ($\Delta\varepsilon = -3.7$), are also measured and their γ_1/K_{22} values are found to be 18.87 and 18.32 $\mathrm{ms}/\mu\mathrm{m}^2$, respectively. Meanwhile, we also plot the γ_1/K_{22} values for various positive LCs with the blue dots. All the measured materials have $\Delta n \sim 0.1$ and clearing point around 80 °C, which is intended for practical applications.

From Fig. 6, for both positive and negative LCs, as $\Delta\varepsilon$ decreases (fewer polar component) γ_1/K_{22} gets smaller as well, leading to a faster response time. But the tradeoff is increased voltage. Therefore, a delicate balance between response time and operation voltage has to be taken into

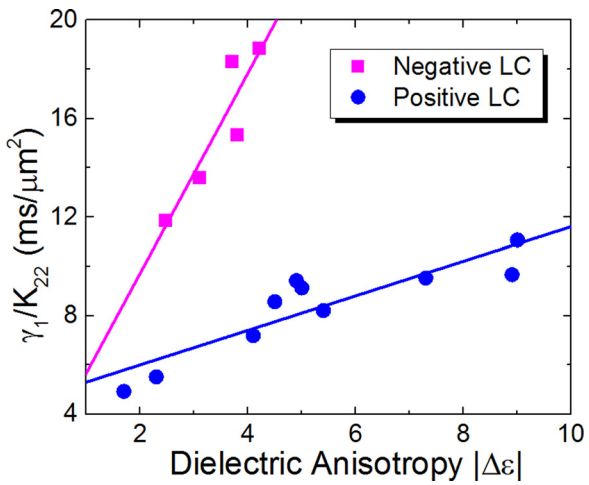

FIG. 6. Visco-elastic coefficient vs. $|\Delta\varepsilon|$ of some LC mixtures with $\Delta n \sim 0.1$ and clearing point around 80 °C.

account simultaneously for material design. The optimal $|\Delta\varepsilon|$ value depends on the intended operation voltage. For both IPS and FFS modes, the strategy is to use a minimally acceptable $|\Delta\varepsilon|$ in order to take advantages of small viscoelastic coefficient.

IV. CONCLUSION

We have developed a semi-empirical equation to calculate the optical decay time of IPS and FFS modes, in which the electric field is not uniform. The model is confirmed by experiment. Afterwards, we apply this simple equation to measure the K_{22} of LC materials. The measured results of 5CB at different temperatures agree well with literature values. Thus, this semi-empirical equation can be used to describe the response time of IPS and FFS cells and it provides a simple yet accurate method to measure the twist elastic constant of LC mixtures.

ACKNOWLEDGMENTS

The authors are indebted to AU Optronics (Taiwan) and AFOSR for the financial supports under Contract No. FA9550-14-1-0279.

[1]M. Schadt, Annu. Rev. Mater. Sci. **27**, 305 (1997).
[2]E. Lueder, *Liquid Crystal Displays: Addressing Schemes and Electro-Optical Effects* (Wiley, Chichester, UK, 2001).
[3]Z. Luo, D. Xu, and S. T. Wu, J. Disp. Technol. **10**, 526 (2014).
[4]M. Schadt and W. Helfrich, Appl. Phys. Lett. **18**, 127 (1971).
[5]M. Schadt, Jpn. J. Appl. Phys. **48**, 03B001 (2009).
[6]M. F. Schiekel and K. Fahrenschon, Appl. Phys. Lett. **19**, 391 (1971).
[7]A. Takeda, S. Kataoka, T. Sasaki, H. Chida, H. Tsuda, K. Ohmuro, Y. Koike, T. Sasabayashi, and K. Okamoto, SID Int. Symp. Digest Tech. Pap. **29**, 1077 (1998).
[8]W. Kiefer, W. Weber, M. Windscheidt, and G. Baur, in *Proceedings of IDRC'92* (1992), p. 547.
[9]M. Oh-e and K. Kondo, Appl. Phys. Lett. **67**, 3895 (1995).
[10]M. Oh-e and K. Kondo, Liq. Cryst. **22**, 379 (1997).
[11]H. Hong, H. Shin, and I. Chung, J. Disp. Technol. **3**, 361 (2007).
[12]S. H. Lee, S. L. Lee, and H. Y. Kim, Appl. Phys. Lett. **73**, 2881 (1998).
[13]Y. Chen, Z. Luo, F. Peng, and S. T. Wu, J. Disp. Technol. **9**, 74 (2013).
[14]D. H. Kim, Y. J. Lim, D. E. Kim, H. Ren, S. H. Ahn, and S. H. Lee, J. Infor. Dis. **15**, 99 (2014).
[15]P. Pieranski, F. Brochard, and E. Guyon, J. Phys. **34**, 35 (1973).
[16]D. K. Yang and S. T. Wu, *Fundamentals of Liquid Crystal Devices*, 2nd ed. (Wiley, Chichester, 2014).
[17]D. Xu, F. Peng, H. Chen, J. Yuan, S. T. Wu, M. C. Li, S. L. Lee, and W. C. Tsai, J. Appl. Phys. **116**, 193102 (2014).
[18]H. Wang, T. X. Wu, X. Y. Zhu, and S. T. Wu, J. Appl. Phys. **95**, 5502 (2004).
[19]H. Gruler, T. J. Scheffer, and G. Meier, Z. Naturforsch. A **27**, 966 (1972).
[20]P. R. Gerber and M. Schadt, Z. Naturforsch. A **35**, 1036 (1980).
[21]S. Faetti, M. Gatti, and V. Palleschi, J. Phys., Lett. **46**, L881 (1985).
[22]F. M. Leslie and C. M. Waters, Mol. Cryst. Liq. Cryst. **123**, 101 (1985).
[23]F. Yang, J. R. Sambles, and G. W. Bradberry, J. Appl. Phys. **85**, 728 (1999).
[24]E. P. Raynes, C. V. Brown, and J. F. Stromer, Appl. Phys. Lett. **82**, 13 (2003).
[25]P. D. Brimicombe, C. Kischka, S. J. Elston, and E. P. Raynes, J. Appl. Phys. **101**, 043108 (2007).
[26]J. L. Volakis, A. Chatterjee, and L. C. Kempel, *Finite Element Method Electromagnetics* (IEEE Press, Piscataway, 1998).
[27]D. Xu, Y. Chen, Y. Liu, and S. T. Wu, Opt. Express **21**, 24721 (2013).
[28]Y. Chen, F. Peng, T. Yamaguchi, X. Song, and S. T. Wu, Crystals **3**, 483 (2013).
[29]X. Nie, R. Lu, H. Xianyu, T. X. Wu, and S. T. Wu, J. Appl. Phys. **101**, 103110 (2007).
[30]J. H. Lee, D. J. Lee, S. W. Oh, M. K. Park, K. H. Park, B. K. Kim, and H. R. Kim, SID Int. Symp. Digest Tech. Pap. **45**, 314 (2014).
[31]S. K. Hao, C. Y. Chiu, Y. Z. Wu, F. Zhao, Y. J. Song, Z. M. Deng, C. Y. Lee, C. C. Luo, and A. Lien, SID Int. Symp. Digest Tech. Pap. **45**, 1414 (2014).
[32]P. G. de Gennes, *The Physics of Liquid Crystals* (Clarendon, Oxford, 1974).
[33]N. V. Priezjev and R. A. Pelcovits, Phys. Rev. E **62**, 6734 (2000).
[34]A. A. Sonin, *The Surface Physics of Liquid Crystals* (Gordon and Breach, New York, 1995).
[35]P. A. Breddels and J. C. H. Mulkens, Mol. Cryst. Liq. Cryst. **147**, 107 (1987).
[36]M. Hara, J. I. Hirakata, T. Toyooka, H. Takezoe, and A. Fukuda, Mol. Cryst. Liq. Cryst. **122**, 161 (1985).
[37]M. J. Bradshaw and E. P. Raynes, Mol. Cryst. Liq. Cryst. **72**, 35 (1981).
[38]I. Haller, Prog. Solid State Chem. **10**, 103 (1975).
[39]S. T. Wu, Phys. Rev. A **33**, 1270 (1986).
[40]J. Li and S. T. Wu, J. Appl. Phys. **95**, 896 (2004).
[41]S. Gauza, X. Zhu, W. Piecek, R. Dabrowski, and S. T. Wu, J. Disp. Technol. **3**, 250 (2007).
[42]D. Xu, L. Rao, C. D. Tu, and S. T. Wu, J. Disp. Technol. **9**, 67 (2013).
[43]H. Chen, F. Peng, Z. Luo, D. Xu, S. T. Wu, M. C. Li, S. L. Lee, and W. C. Tsai, Opt. Mater. Express **4**, 2262 (2014).
[44]D. Xu, H. Chen, S. T. Wu, M. C. Li, S. L. Lee, and W. C. Tsai, J. Disp. Technol. **11**, 353 (2015).
[45]H. Chen, M. Hu, F. Peng, J. Li, Z. An, and S. T. Wu, Opt. Mater. Express **5**, 655 (2015).